Microchemical Journal 206 (2024) 111353

Contents lists available at ScienceDirect

Microchemical Journal

journal homepage: www.elsevier.com/locate/microc

Diagnosis of archaeological bones: Analyzing the state of conservation of lower Pleistocene bones through diagenesis methods

Andrea Díaz-Cortés [a,b,*], Héctor Del Valle [a,b], Lucía López-Polín [a,b], Jorge Otero [c], Isabel Cáceres [a,b], Noé Valtierra [a,b], Antonio Pineda [a,d], Palmira Saladié [a,b,e], Josep Vallverdú [a,b,e]

[a] Institut Català de Paleoecologia Humana i Evolució Social (IPHES), Zona Educacional 4, Campus Sescelades URV (Edifici W3), 43007 Tarragona, Spain
[b] Universitat Rovira i Virgili, Departament d'Història i Història de l'Art, Avinguda de Catalunya 35, 43002 Tarragona, Spain
[c] Universitat de Barcelona. Department d' Arts i Conservació-Restoratió. Facultad de Bellas Artes. Carrer de Pau Gargallo, 4, Les Corts, 08028 Barcelona
[d] UMR 7194 HNHP (MNHN-CNRS-UPVD), Département Homme et Environnement, Muséum National d'Histoire Naturelle. 1 rue René Panhard, 75013, Paris, France
[e] Unit Associated to CSIC, Departamento de Paleobiología. Museo Nacional de Ciencias Naturales, C/ José Gutiérrez Abascal, 2, 28006, Madrid, Spain

ARTICLE INFO

Keywords:
Cultural Heritage
Archaeological bones
Fossil
Diagenesis
Conservation diagnosis
Bioapatite

ABSTRACT

Initial physicochemical assessment of cultural materials plays a critical role in the research and management of cultural heritage, serving as a foundation for comprehending deterioration mechanisms and developing effective conservation treatments. However, this knowledge is more advanced in several cultural materials such as artwork or historic buildings, than in bone and fossils. This study focuses on bone material conservation, applying diagenetic methods for characterizing and assessing the state of conservation of archaeological bones from Pit 1 at Barranc de la Boella (BB), an open-air archaeological site from the late Early Pleistocene, from a conservation perspective.

Microstructural analyses, including mercury intrusion porosimetry (MIP) and histological analysis, alongside microchemical analyses through Attenuated Total Reflection Fourier Transform Infrared (ATR-FTIR), and FTIR with KBr pellets and X-ray Diffraction (XRD), were conducted to evaluate the decay processes affecting the bones. Results indicated poor bone preservation characterized by high porosity, significant microbial attack, collagen degradation, and the potential recrystallization of bioapatite into fluorapatite. These findings underscore the substantial challenges presented by open-site conditions to preservation efforts and highlight the need for suitable conservation treatments, such as consolidation to reinforce the microstructure.

The study emphasizes the importance of characterizing archaeological bones to understand the factors influencing their preservation states and guide conservation works in this material. This work contributes to the knowledge of diagenesis studies to standardize the diagnosis of the state of conservation on archaeological bones.

1. Introduction

Conservation field involved a wide variety of materials e.g., [1–3]. Recent decades have seen significant development in the research of several heritage materials beyond traditional art objects, by scientific studies and manuals e.g., [4–7]. Thorough diagnostic analyses conservation professionals determine the composition and assess the state of conservation, exploring the decay causes and mechanism. This is better understood in limited materials like artworks and building heritage than in materials such as archaeological bones [8–11]. This expansion, however, has led to a substantial imbalance in knowledge across different cultural heritage materials.

Bone material conservation, frequently found in archaeological and paleontological contexts, has received comparatively less attention. Published research has focused on other areas of research which include:

- Conservation practices focus on treating bones as information sources for archaeology and paleontology research. Consequently, treatments are primarily evaluated based on their non-intrusive nature to these research activities, while simultaneously enhancing the mechanical properties of the bones for examination and handling [12–15]

* Corresponding author.
E-mail address: adiaz@iphes.cat (A. Díaz-Cortés).

https://doi.org/10.1016/j.microc.2024.111353
Received 18 April 2024; Received in revised form 10 July 2024; Accepted 2 August 2024
Available online 6 August 2024

Fig. 1. Fig. 1. a) Image of Pit 1 at Barranc de la Boella site, 2019, b) Femur belonging to *Mammuthus meridionalis* recovered at Pit 1, c) Samples from Pit 1.

- The side effects of conservation treatments, often involve cleaning and consolidation methods that can negatively modify bone surfaces ex.[16–20]. These alterations can impact critical analyses such as isotope analysis [21–26], radiocarbon dating [27,28] or DNA extraction [29–31].
- The evaluation of the effectiveness of traditional consolidation products, such as organic polymers [32,33], and innovative for the consolidation of bones such as $Ca(OH)_2$ nanoparticles [34] or diammonium phosphate [28,31,35]

These studies provide a qualitative and brief description of the initial state of conservation, which depends directly on the individual experience of the conservation professional. In general, archaeological conservation literature, is simplistically categorized as organic materials, yet there is a significant variation among them, ranging from modern bones to fossilized ones, attributable to extensive periods of burial. conservators and conservation scientists often find themselves repurposing research methodologies initially developed for different materials, under the assumption that these quantitative methods are universally applicable. Despite presenting quantitative data, such as porosity figures, this research falls short in providing the necessary context; it does not explain whether the provided data indicate a state of poor conservation, a practice that contrasts sharply with the well-established standards for evaluating other cultural materials like monumental stone. Notably, Ferreira Pinto and Delgado Rodrigues (2008) [36] highlighted the importance of porosity in stone consolidation, noting that if porosity is below 18 %, those stones present a good state of preservation. This is significant because every conservation study on such materials systematically employs a petrography analysis that reveals the physicochemical characteristics of brittle stones, such as Maastricht limestone [37–39], Globigerina limestone from Malta [40–43] or the Ança limestone from Portugal.

As noted in previous work [44], there is a lack of systematic studies on bone preservation, which is crucial for assessing the necessity of conservation treatments. Consequently, the diverse chemical compositions of bones that have undergone burial processes remain underexplored in previous conservation studies eg. [20,31,32,34,44–47]. The absence of systematic studies in the conservation field leads to a limited understanding of the mechanisms and effects of deterioration in archaeological bones. Consequently, variables that may affect the efficacy of different bone conservation and restoration treatments are not well-documented.

To begin developing and contributing to the knowledge about bone conservation, taphonomy can help us overcome this gap [48–53]. Taphonomy focuses on modifications of bones which start at the time of death identifying mainly two phases bioestratinomy (remain deposition) and fossildiagenesis (burial phase) [54,55]. Taphonomic studies, although not widely disseminated in the field of conservation, can significantly enhance our understanding of the nature and deterioration of skeletal remains and aid in developing strategies for both heritage management and bone conservation treatments [56–58]. Within taphonomy, bone diagenesis studies examine the changes bones undergo during the burial phase.

Commencing in the mid-20th century, diagenesis research has predominantly aimed at bone characterization to support analyses of paleoenvironments and paleodiets ex. [59–64]. Therefore, it is important to distinguish between the terms “conservation” and “preservation” because they are used differently in this work compared to their meanings in the cultural conservation field. In diagenetic studies, these terms are employed to denote the preservation of valuable data relating to the environment and isotopes, essentially highlighting how bones maintain their original state without undergoing any chemical changes throughout their taphonomic journey ex. [65–68]. Meanwhile, in conservation, these terms relate to a specimen’s stability for safe extraction and handling [12,69].

Bone, as a biological composite material, consists of a mineral fraction (bioapatite) and an organic matrix, primarily composed of collagen. During taphonomic phases, bones experience several changes, including the hydrolysis of collagen and the recrystallization of the mineral part, influenced by environmental conditions (pH, hydrology regime, etc.) and microbial activity, which can also lead to the destruction of their morphological structure [70–73]. These processes can result in a wide spectrum of bone preservation, from complete destruction, as seen in many archaeological sites, to a completed mineral interchange [74].

Far from the goal of conducting diagenetic studies to understand how the site was formed, the focus of this research is to assess the conservation of ancient bone remains from the Lower Pleistocene, particularly those excavated from Pit 1 at Barranc de la Boella. These remains have been previously recognized for their extremely poor preservation, which is not the average of archaeological bone preservation, and these remains need internal reinforcement measures to ensure their future preservation. To achieve this, we will use both the analysis of the preservation of their microstructure and the physicochemical characterization of the samples. These insights are invaluable in the decision-making process related to archaeological conservation. Moreover, this study will contribute to the knowledge about this type of material in the field of cultural heritage conservation and will serve as a foundation for future research in this area. Additionally, it will provide valuable information on the preservation of these bones for fields such as DNA extraction, datings, and isotopic analysis.

2. Materials and methods

2.1. Archaeological bone samples: Barranc de la Boella

Archaeological bones from Pit 1 at Barranc de la Boella (BB), La Canonja, Tarragona, Spain, were used in this study. BB is an open-air archaeological site situated in a fluvial deltaic environment (Fig. 1 a), where water significantly influenced the site’s formation. Fieldworks at BB have been developed three different pits called Pit 1 (P1), La Mina, and El Forn. Bones from BB presented a poor surface preservation due to taphonomic processes, which have posed significant challenges in previous taphonomic studies [75–77]. Here, samples belonging exclusively to a *Mammuthus meridionalis*’ femur recovered in layer 2 of Unit II in Pit 1 were included (Fig. 1 b and c). Pit 1 is interpreted as a *butchering site* [78] and Unit II was placed in the late Early Pleistocene (1.0–0.8 Ma)

Table 1
Principal ATR-FTIR peak position, ratio and baselines.

Vibrational mode	Maximum peak position	Baseline
Amide I	1630–1700	1710–1590 cm^{-1}
v_3PO_4	1035	1150–890 cm^{-1}
v_4PO_4	605, 565	750–420 cm^{-1}
v_3CO_3	1420	1720–1290 cm^{-1}
v_4CO_3	712	730–700 cm^{-1}
Ratio	**Parameter calculation**	
Amide I/PO_4	[(1630–1700) /1035]	
Nitrogen (%wt)	20.6 (Amide I /1035) + 0.31	
Collagen (%wt)	113.13 (Amide I/1035) + 1.69	
IRSF	[(565 + 605) /590]	
Cal/PO_4	712/1035	

through biostratigraphy, paleomagnetism, and cosmogenic nuclide methods [78,79]. Unit II lithofacies, characterized by its poorly stratified sands and gravels, indicates subaerial and subaquatic mass flow deposits, commonly described in alluvial fan and fan-delta sedimentary environments.

2.2. Multimethod approach for characterizing and assessing the state of conservation of archaeological bones: A proposal

2.2.1. Microstructural analysis

2.2.1.1. Mercury intrusion porosimetry. Total pore volume and pore size distribution of samples from BB were determined using mercury intrusion porosimetry (MIP). This was performed with an Autopore III 9410 porosimeter (Micromeritics, Norcross, US), located at the Department of Mineralogy and Petrology at the University of Granada (UGR), capable of measuring pores ranging from 0.003 to 360 μm in diameter. Approximately 1 g of bone of 3 samples from BB was prepared, which involved oven-drying for 48 h at 60 °C before analysis [80].

2.2.1.2. Thin section: Histological analysis. For histological analysis, a 30 μm thick bone section was prepared and examined under transmitted and polarized light [73,81], using OLYMPUS-BX and Carl Zeiss Jenapol-U microscopes at the Department of Mineralogy and Petrology at the University of Granada (UGR) and Laboratory of Geoarchaeology at Institut Catalá de Paleoecologia Humana i Evolució Social (IPHES-CERCA), respectively. In addition to optical microscopy, Environmental Electro Scanning Microscopy (ESEM) analysis was conducted using the Phenom-XL G2 Desktop SEM microscope at the Department of Mineralogy and Petrology at UGR. Carbon coating was not required, with parameters set according to the working distance: the voltage varied from 10 to 20 kV, operating in a low-pressure vacuum. Elemental analysis was conducted in areas of interest to describe the state of preservation [72].

The Oxford Histological Index (OHI) was used to evaluate the degree of histological preservation on a scale from 0 (poor preservation) to 5 (well-preserved) [48,82,83]. Analysis of data from Jans 2005 [79; Appendix: Site Description and Results; pp, 105–151] was presented, showing different qualitative data obtained from the histological analysis, considering the OHI, and the presence or absence of tunnels generated by bioerosion. With this data, a Confidence Region for Multiple Correspondence Analysis (MCA) was conducted using the R software [84], with the 'cabootcrs' R library [85] to relate the preservation to the archaeological context and chronologies.

2.2.2. Chemical analysis

2.2.2.1. Attenuated total reflection Fourier Transform infrared (ATR-FTIR). FTIR analysis with KBr were examined in 3 samples, in order to compare to ATR-FTIR samples. Spectra were collected using a Jasco 6700 spectrometer in the 4000 − 400 cm^{-1} range at Scientific and Technical Service at University of Rovira i Virgili (URV) Spectra KBr were an average of 200 scans at a resolution of 2 cm^{-1}. The pellets were produced by compression of the powder in a stainless steel die of 13 mm at 9 tons for about 20 s using a manually operated hydraulic press.

Chemical analysis was conducted using ATR-FTIR. A total of 7 samples were ground into a homogeneous powder with particle sizes ranging from 50 to 20 μm. These spectra are averages of 64 scans recorded in absorbance mode at a resolution of 4 cm^{-1}. The anvil pressure on the ATR crystal was adjusted to achieve an absorbance of 0.5 for the $\nu_3(PO_4^{3-})$ band around 1035 cm^{-1} [86]. The spectra were then analyzed with Spectra Manager software to extract ratios, using the baseline established in previous bone diagenesis studies [70–76].

Parameters for analyzing organic and mineral content were determined using different ratios, summarized Table 1. This table describes these parameters and the baselines as reported in later studies [87,88].

The 2nd derivative analysis was conducted to improve spectral resolution. This analysis was processed by Spectra Manager software, applying the Savitzky-Golay method for the 2nd derivative analysis with a 3rd order polynomial and 9 smoothing points, specifically for observing apatite spectra [89,90]. The wavenumber ranges observed where:

- 640–540 cm^{-1}: Modern bones exhibit two intense peaks at 600 cm^{-1} and 560 cm^{-1}. During bioapatite modification in fossilization, an additional peak between 573–575 cm^{-1} emerges, its intensity increasing with the degree of fluorination.[90].
- 1000–940 cm^{-1}: A shift of the 960 cm^{-1} peak to higher frequencies indicates changes in the crystal lattice strain, potentially due to decreased carbonate content or fluoride ion incorporation [89].
- 900–840 cm^{-1}: Peak 866 cm^{-1} ($\nu_2(CO_3)$) in the second derivative produces three bands, with the 865 cm^{-1} band being the most intense. This finding is related to labile carbonates in bioapatite. The analysis also highlights the presence of B-type and A-type carbonates at 873 cm^{-1} and 880 cm^{-1}[90,91]. Studying their intensities provides more information due to the contribution of each carbonate, in addition to the bands from the un-derived spectra corresponding to the frequencies of $\nu_3(CO_3)$.

2.2.2.2. X-ray diffraction (XRD). Mineralogy and crystallite size/strain of BB samples were determined using XRD technique. These analyses were conducted on a Philips PW-1710 diffractometer equipped with an automatic slit, and on an XPert Philips with a Ni filter at the Department of Mineralogy and Petrology at UGR. The measurement parameters included Cu Kα radiation (λ = 1.5405 Å), 45 kV, 40 mA, an exploration range of 4 to 70° 2θ, step sizes of 0.001° 2θ, and a goniometer speed of 0.01° 2θ/s. Powder samples were placed in zero-background Si sample holders. Mineral phases were identified by comparing them with JCPDS powder spectra.

Quantitative phase analysis of apatite crystals was performed using the Rietveld method and XPowderX software, employing the Scherrer equation to calculate the average crystallite size: D (0 0 2) = Kλ/(B cos θ), where K is a constant that varies with the crystalline habit, selected as 0.9 for elongated apatite crystals, λ is the wavelength of CuKα radiation (λ = 1.5406 Å), B is the full width at half maximum (FWHM) of the (0 0 2) apatite diffraction peak, and θ is the corresponding diffraction angle for this reflection. XRD line width helps determine the average size of coherent crystal domains and serves as a measure of the material's crystallinity.

Through Rietveld analysis [92], the a-axis, c-axis, and cell volume of the BB samples were determined. Models for fluorapatite and hydroxyapatite were taken from [90,91].

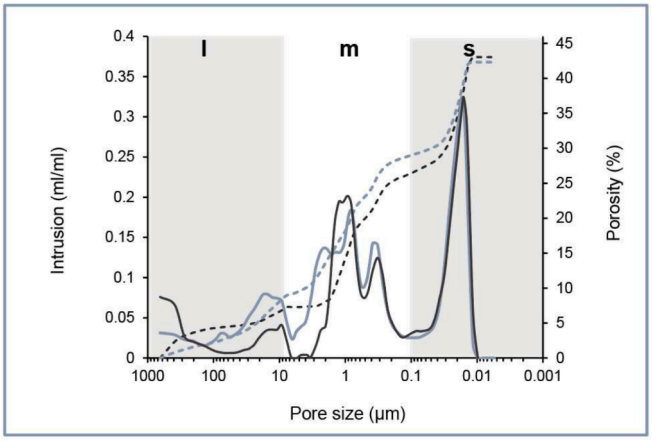

Fig. 2. Pore size distribution and total porosity (%) of Pit 1, of two samples (continuous line). Cumulative Porosity (%) (Dasheded line).

3. Results

3.1. Microstructural analysis

3.1.1. MIP

MIP results have exhibited a three-modal porosity structure following the classification by Turner-Walker et al. (2002), the smallest pores are denoted as "s" (<0.1 μm), medium pores as "m" (0.1 μm − 10 μm), and the largest pores as "l" (>10 μm) **(**Fig. 2**).**

The average porosity of the samples is between 42–43 %, with specific values of 0.3629 ml/g (42.32 %) and 0.3308 ml/g (43.02 %). When compared to data from Nielsen-Marsh and Hedges (1999)[80], which indicates that the total porosity of a modern bone is 0.0445 ml/g, these samples exhibit significantly higher porosity. Additionally, the density measurements show low values, with the bulk density recorded at 1.23 g/mL and the skeletal density at 2.15 g/mL.

MIP data indicate a significant presence of tunnel-like pores ranging from 30 μm to 0.1 μm, corresponding to the "m" type. These medium-sized pores are typically associated with microbial attack, linked to microscopic focal destruction (mfd) or Wedl tunnels caused by bacteria or fungi, respectively [48,93,94].

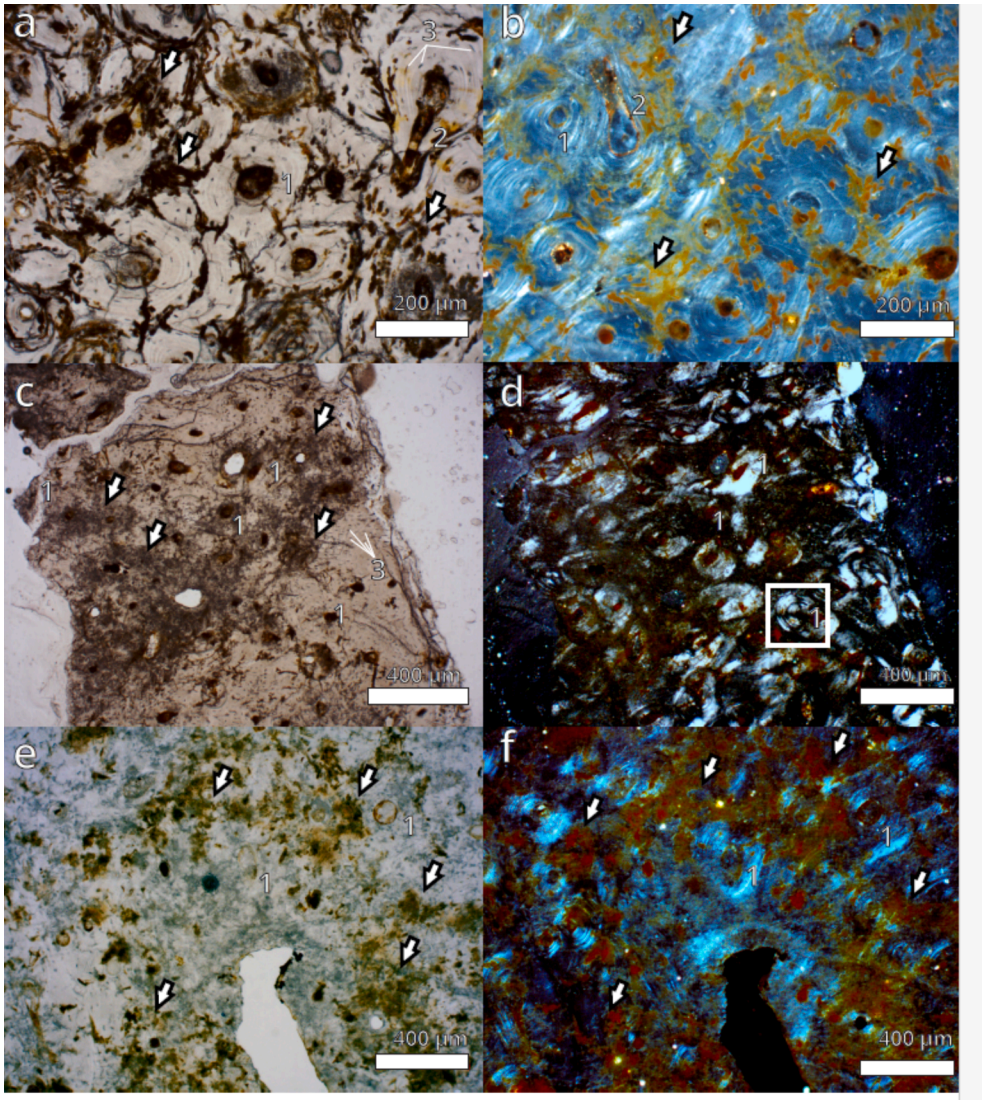

Fig. 3. Thin section images**.** On the left, PPL images, on the right, the same images in XPL. In all of them, 1. Haversian Canal. 2. Volkman's Canal. 3. Osteocytes. a) and b) Images of a well-preserved area, with some bioerosion. c) and d) Image of an area with evident bioerosion (arrows point to deteriorated areas), the box highlights an osteon with the "Maltese Cross" effect. e) and f) Images of an area with low preservation (arrows indicate areas of alteration).

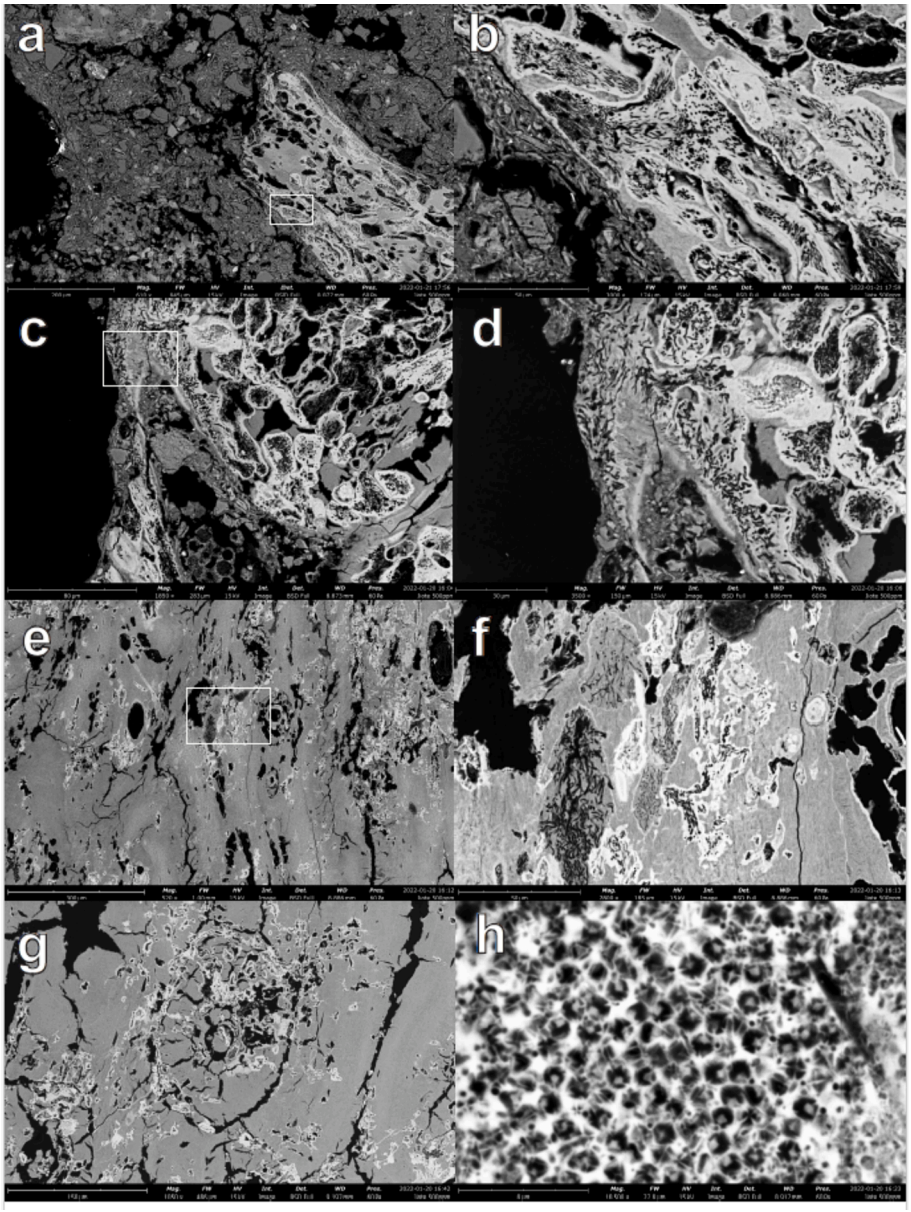

Fig. 4. ESEM images of thin sections. a-f) Areas showing *mfd*, with remineralized and demineralized areas. g) Detail of an osteon with mfd, h detail of the tunnels generated by bioerosion.

Furthermore, the MIP graphs show a notable representation of "s" type pore sizes smaller than 0.1 μm. These smallest pores are often connected to the loss of collagen [48,74,80,95].

Table 2
ATR-FTIR results of organic and biomineral of archaeological bones from Pit 1 (Barranc de la Boella) samples.

	Organic fraction			Mineral fraction		
	Amide I/ PO_4	N wt %	Collagen wt %	CO_3/ PO_4	IRSF	ν1 PO4 (cm-1)
BB1	0.01	0.54	2.95	0.15	4.65	965.61
BB2	0.01	0.54	2.98	0.16	4.72	965.61
BB3	0.01	0.59	3.21	0.15	4.65	965.61
BB4	0.01	0.58	3.17	0.19	4.49	965.61
BB5	0.02	0.65	3.58	0.19	4.61	965.13
BB6	0.01	0.57	3.14	0.18	4.74	965.61
BB7	0.01	0.62	3.38	0.18	4.61	965.61
Mean	0.01	0.59	3.20	0.17	4.64	965.53
S.D.	0.00	0.04	0.22	0.02	0.08	0.18

3.1.2. Thin section

Two samples were examined, all displaying signs of bioerosion, commonly referred to microscopical focal destructions (mfd).

The typical structures of bone are difficult to see in some images Fig. 3**.a-b** (Haversian canals, with osteocytes in lacunae surrounding them, shown in). However, some samples show fractures crossing the osteons and radial fissures within them. The structural destruction of the histological structure is evident through the diffusion of a stain displaying grey, black, and copper (Fig. 3 **c-f**). Under cross-polarized light (XPL), these areas lose the characteristic birefringence of well-preserved histological structures **(**Fig. 3**. d, f**).

ESEM allowed observing thin sections under higher magnification. Several regions were identified as characterized by varying coloration – notably, whiter, and grayish zones **(**Fig. 4 **a-c**). Within the white regions, the presence of tunnels ranging from 5 to 10 μm in thickness was observed (Fig. 4**. d-h**). These channels are likely indicative of bioerosion, which is known to cause remineralization of the bone [93,94,96]. This process results in the formation of hypermineralized

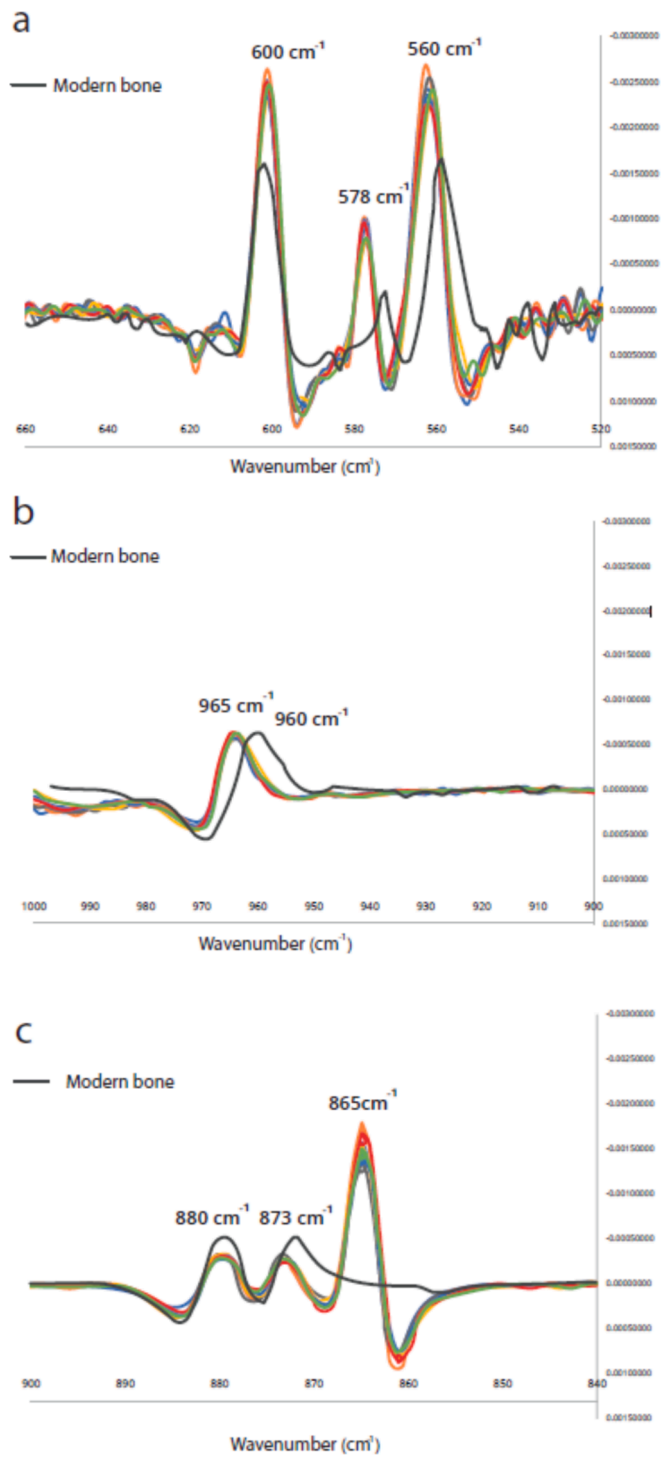

Fig. 5. ATR-FTIR spectra 2nd derivative from the Pit 1 samples comparing to modern bone a) ν_2 (PO_3) region (500 cm^{-1}–650 cm^{-1}) b) ν_1(PO_4) region (960 cm^{-1}) c) ν_3(CO_3) region (between 840 cm^{-1}-900 cm^{-1}).

areas alongside demineralized regions [73,93,97,98].

Oxford Histological Index (OHI) observed in the sample slides from BB ranges between grades 0 and 2 because clear structures are not visible, and only the Haversian canal can be identified [82].

3.2. Chemical analysis

3.2.1. ATR-FTIR

BB samples results of the organic and mineral fraction of 7 samples are summarized Table 2. 2nd derivate spectra are exposed in Fig. 5.

Lebon et al. (2016) exposed an equation which allow to calculate the percentage of N% greater than 0.5 % to determine the relative amount of collagen in the sample [86]. Table 2 describes the percentages of N (%) and collagen (%) that have been calculated for each sample. Results have shown a relatively low percentage of 3 % on BB samples.

On the other hand, in the mineral part, the carbonate and phosphate index decreases compared to the data from modern bone. It is important to highlight that no signal of secondary calcium carbonate is observed, and therefore, it cannot be considered the calculation of calcite (%)[88]. IRSF increases to 4.64 compared to the data presented from modern bone, which usually ranges between 3–3.5.

Second derivate analysis also exposed the absorption band at 578 cm^{-1} **(**Fig. 5**.a),** along with bands at 600 cm^{-1} and 560 cm^{-1}, suggesting a high incorporation of fluorine into part of the bioapatite, following the observations of Margariti et al. (2019)[90]. Furthermore, there is a shift in the phosphate band from 960 cm^{-1} to higher frequencies (965 cm^{-1}) (Fig. 5**.b)**, indicating a decrease in tension and changes in crystal order due to the incorporation of certain ions, according to Lebon et al. (2010) [89]. Significantly, the band at 560 cm^{-1} associated with $\nu_3(CO_3)$ has increased, reflecting a considerable presence of labile carbonates **(**Fig. 5**. c)**. This phenomenon aligns with the observed increase in the IRSF. In addition, the bands corresponding to Type B and Type A carbonates are very similar, indicating that there is no clear predominance of any carbonates types, contrary to the usual case where Type B carbonates usually is higher [90,91].

3.2.2. XRD

Crystallite size mean is 14.75 nm (±1.25) for a-axis and 36 nm (±2.65 nm) for c-axis. The crystallographic parameters of unit cell of 3 BB samples are 525.45 $Å^3$ (±0.09 $Å^3$) for volume cell, 9.38 Å (±0.0007 Å) for a-axis (Å), and 6.90 Å (±0.0004 Å) for c-axis. Fig. 6 illustrates a plot of the BB data overlaid on reference data, where samples align with the fluorapatite reference [90,91].

4. Discussion

Results regarding porosity, and the organic or inorganic bone fractions, enable a quantitative understanding of the changes, alteration processes, and the conservation state of the BB samples. Furthermore, these findings allow for comparisons with other archaeological bones data, supporting in the contextualization of BB preservation state.

4.1. Organic fraction: Hydrolysis and loss of collagen

Thin sections observation has allowed to observe poor preservation. The loss of birefringence indicates that the collagen-bioapatite fibers are undergoing modifications, and their orientation is being altered[73].

Moreover, the significant presence of 's' pores (less than 0.1 μm) is primarily associated with the loss of collagen fibers, which correspond to this diameter size. High contribution of 's' pores might be common for fossilization because of pores filling with minerals or forming secondary minerals within the bone, but the chemical analysis corroborated this loss of collagen [74].

Amide I/ PO_4 confirms the reduction of collagen, aligning with the findings from MIP that indicate the presence of 's' type pores. Fossilization is generally perceived as occurring under stable conditions, wherein collagen reduces gradually through chemical hydrolysis [99,100]. However, under certain circumstances, this process can accelerate. Alkaline environments further weaken collagen's structure. Previous works note that some burial process involving quicklime raise the pH and accelerated collagen loss [56]. Conversely, organic matter decomposition produces acids, reducing mineral dissolution but potentially causing collagen fiber hydrolysis and swelling. Therefore, the organic fraction of bone is far more vulnerable in any burial condition compared to the mineral fraction.

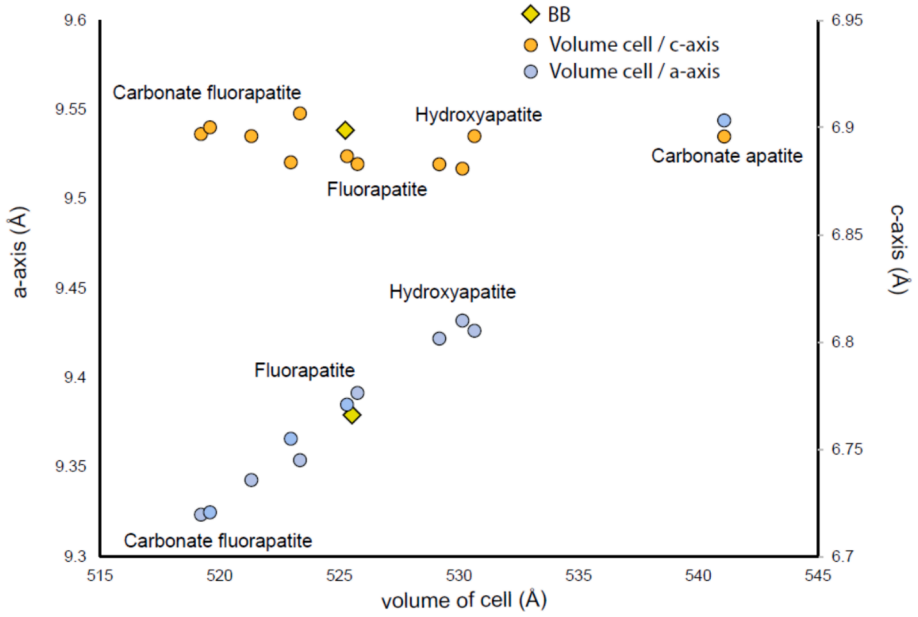

Fig. 6. The relationship between the crystallographic c-axis (right) and a-axis (left) with the unit cell volume is demonstrated for the bones and selected reference materials examined, based on data sourced from Stathopoulou et al., 2008 [87]. BB samples unit cell parameters plot close to fluorapatite parameters.

4.2. Microbial attack

Attack by microorganisms can be related to both the loss of organic matter and the increase in porosity, which can occur when bacteria metabolize the organic matter or during post-mortem phases. [48,50,71]. The significant presence of 'm' type pores (5–10 μm), which are associated with microbial attacks, is more pronounced in these samples [73]. This is supported by the analysis of thin sections, both at high magnifications and through ESEM analysis.

Jans (2005)[81] presented images of histological slides from horse and human femurs featuring dark areas that resemble those we have identified and associated them with microbial attacks. These dark zones are classified as "budded" tunnels, which become black due to air retention during the encapsulation process. Moreover, through ESEM thin section observation, the presence of bioerosion is further confirmed, evidenced by tunnels near remineralized areas as illustrated in previous studies [72,93,98,101–103]. Therefore, microbial attack also can affect bioapatite by remineralization processes.

4.3. Mineral fraction: Remineralization and formation of fluorapatite

Mineral bone was analyzed by ATR-FTIR. $\nu_3CO_3^{2-}/\nu_3PO_4^{3-}$ ratio, indicative of bioapatite remineralization and potential introduction of carbonates and reduction of phosphates. This index usually decreases due to carbonate dissolution and substitution by other PO^{-4}. $\nu_3CO_3^{2-}/\nu_3PO_4^{3-}$ is lower compared to studies analyzing modern or more recent bones. In Fig. 7**. a**, these samples are compared with data from other studies regarding this index. Bones, exhibiting good preservation of carbonate quantities relative to phosphates expose values above 0.2, similar to modern bones. Highly mineralized medieval samples from Appigliano (Italy) show an exceptionally low index. [104]. In contrast, cave environment samples like Azokh (Sudan) display very high indices (karst context). Samples from the Miocene show similar indices, below 0.2, but not as low as those from Appigliano, Meteoritic levels of Al-Khaday, which have been documented as bones with low bioapatite preservation and higher remineralization.

IRSF of 4.6 ± 0.08 in the BB samples is higher than in modern or well-preserved bones, suggesting ongoing remineralization. This increase in IRSF is influenced more by burial conditions than the site's chronology (Fig. 7**. b**). Dal Sasso et al. (2016)[88] reported very high IRSF values in recent levels of the open-air site Al-Khiday, but the IRSF of BB samples is not as high. Azokh cave samples show lower IRSF values (3.5–4), likely due to the cave context, as opposed to open-air sites. Cave sites from France like Bize-Tournal, Song Terus, and Orgnac 3 also exhibit a similar crystallinity index to Azokh, reflecting better bone preservation in karstic environments [74,89]. In contrast, Miocene samples have even lower IRSF values than BB [90].

However, authors have concerns about the differences between KBr and ATR-FTIR techniques, in which KBr method may overrepresent $\nu_3CO_3^{2-}/\nu_3PO_4^{3-}$ data and underrepresent IRSF data. These considerations are considered [105] and Fig. 7 illustrates the differences that exist regardless of chronologies. These data suggest that the decrease in the $\nu_3CO_3^{2-}/\nu_3PO_4^{3-}$ ratio or the increase in IRSF is not fundamentally related to the chronological age of the site; rather, the conditions of burial play a crucial role [49,88].

Remineralization and transformation towards a fluorapatite mineral have been observed through second derivative analysis of the infrared spectrum and XRD crystallographic axes and cell volume parameters. On the wavenumber 500–650 cm^{-1}, there is a clear increase in the peak at 578 cm^{-1}, indicating a higher fluoride content in the crystal lattice [90]. The frequency at 960 cm^{-1} shifts to 965 cm^{-1} in the BB samples resulting in a decrease in lattice strain [89]. Therefore, it can be inferred that the BB samples have undergone mineral transformations and could potentially exhibit the introduction of F^- ions in the crystal lattice, resulting so in a phase near to fluorapatite or carbonated fluorapatite [106]. Between 850–900 cm^{-1}, a band at 865 cm^{-1} is observed, which is not present in samples like modern bone. According to Margariti et al. (2019)[90], this band is associated with the presence of labile or unstable carbonates, also found in samples studied from the Miocene. Stathopoulou et al. (2008)[91] link this band to an increase in the crystallinity of bioapatite. Aufort et al. (2019)[107], examined Miocene fossils in Kenya, suggesting that the presence of the labile carbonate band corresponds to mineral carbonated fluorapatite.

XRD analysis confirms the presence of fluorapatite, as shown in Fig. 6. The bioapatite unit cell displays measurements consistent with fluorapatite in the crystal. There has been a notable reduction in the a-axis and cell volume. This reduction of a-axis and cell volume could be related to carbonate introduction, however, according to Margariti et al. (2019) those containing B-type CO_3^{2-} (substituting for PO_4^{3-} in the apatite lattice) reference samples presented less than 9.35 Å for a-axis and

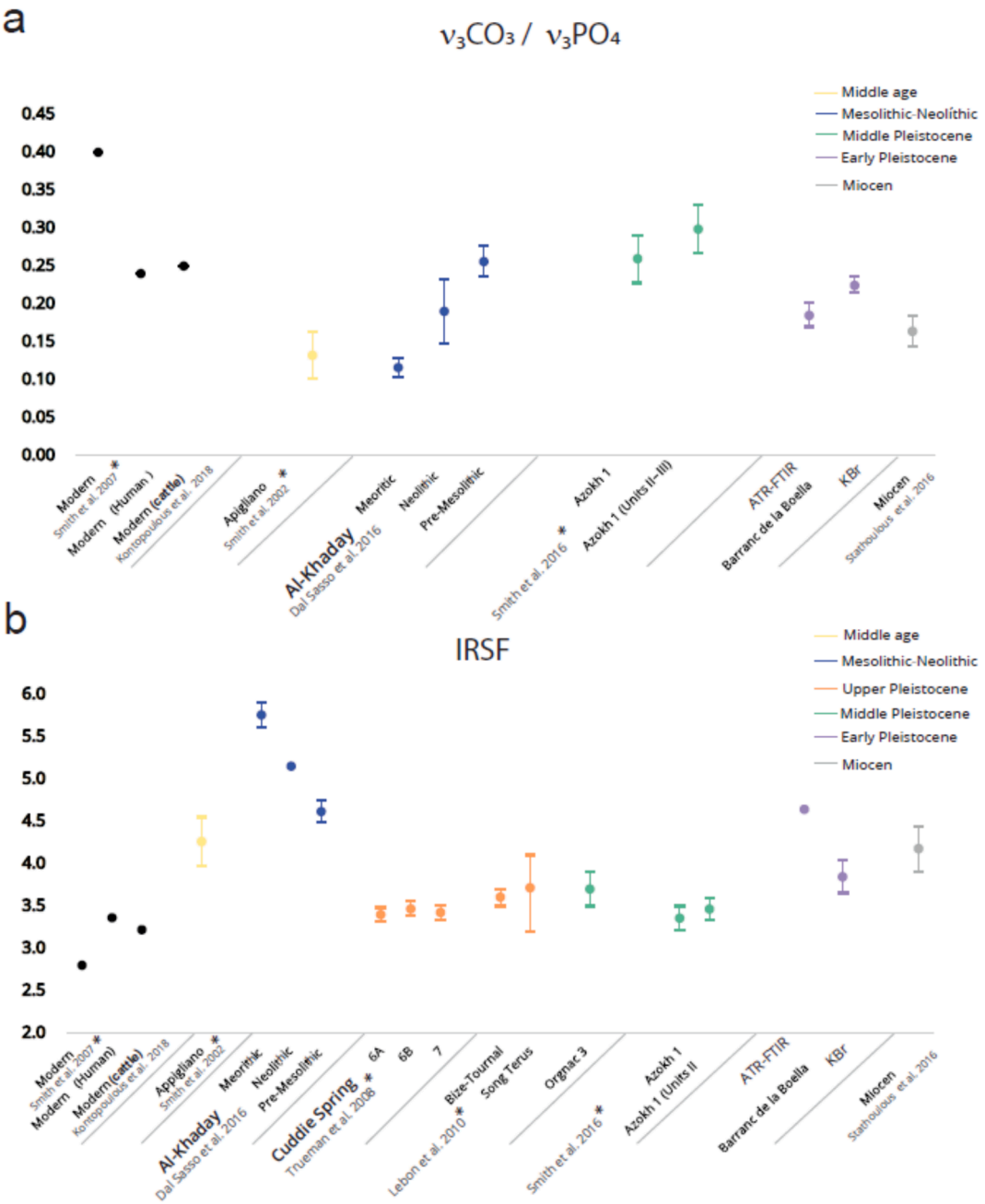

Fig. 7. Confidence intervals of CO_3/PO_4 and IRSF from sites previously published, along with BB samples. (*Indicates KBr FTIR analysis).

around 520 Å^3 for cell volume. This parameter is significantly lower than BB samples which, as it is mentioned in 4.2.2 section corresponds to geological fluorapatite references [91]. This is also previously reinforced by the 578 cm^{-1} peak by second derivate in ATR-FTIR spectra.

This is in line with previous studies that analyzed cell units across paleontological and archaeological sites, from the Triassic to the Holocene[108]. Fig. 8 plots of a-axis and volume cell of Piga et al. 2009 [108] with the data from the BB samples of this study. BB samples are located near Pleistocene samples and a cell unit corresponding to fluorapatite. However, other data from the BB site are closer to Holocene sites from Piga et al. 2009 [108]. This highlights the necessity for detailed contextual information, as it remains ambiguous which of the three BB sites the samples come from. This is important as it may reflect a wide variability of burial environments in different areas of the same site. Cell unit data from all these sites with their burial context would aid in better understanding the transformation that bone bioapatite undergoes and how other analyses could be affected, ex. dating [109].

4.4. State of conservation: Chronology vs. Burial conditions

Generally, conservation literature suggests that the main differences in the preservation state of archaeological bones primarily depend on their chronology. However, it is essential to contextualize these findings to comprehend this preservation state and the wide variability observed in archaeological bones. Previously reported data help improve descriptions of the BB samples' state of conservation and allow comparisons with bones from other chronologies and contexts in published works, highlighting the value of this information in understanding the factors influencing preservation.

According to MIP data from modern bone samples [48,110], an average real density of 1.9 g/ml and an apparent density of 2.1 g/ml have been observed. In the case of the BB samples, decrease in real

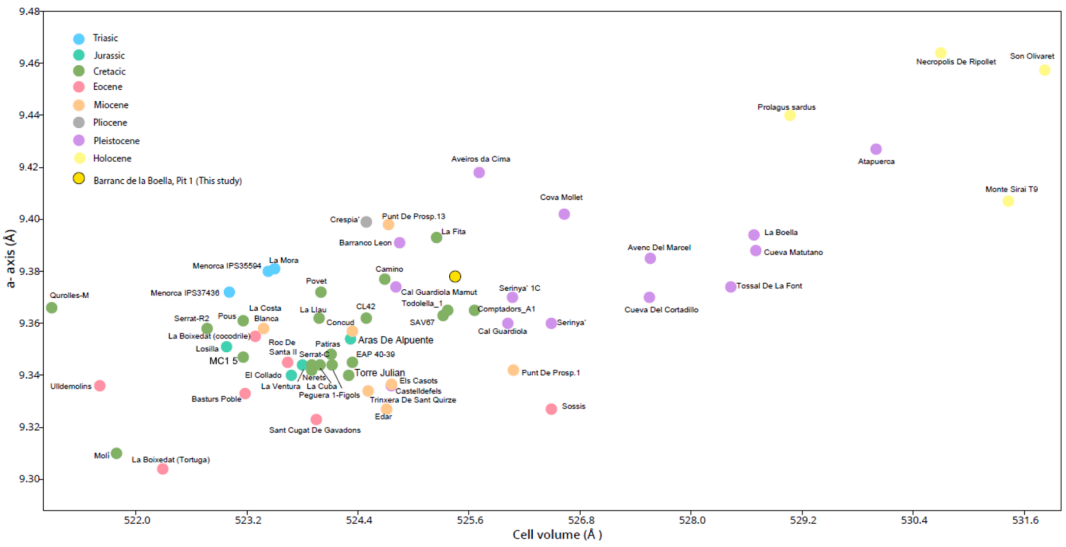

Fig. 8. Relationship between the crystallographic a-axis and unit cell volume is derived from and the current study of Pit 1 at Barranc de la Boella. Samples are divided by the chronologies provided. The BB samples used in this study are from Pit 1 at Barranc de la Boella, while the 'La Boella' data from Piga et al. (2009) lack specific site information.

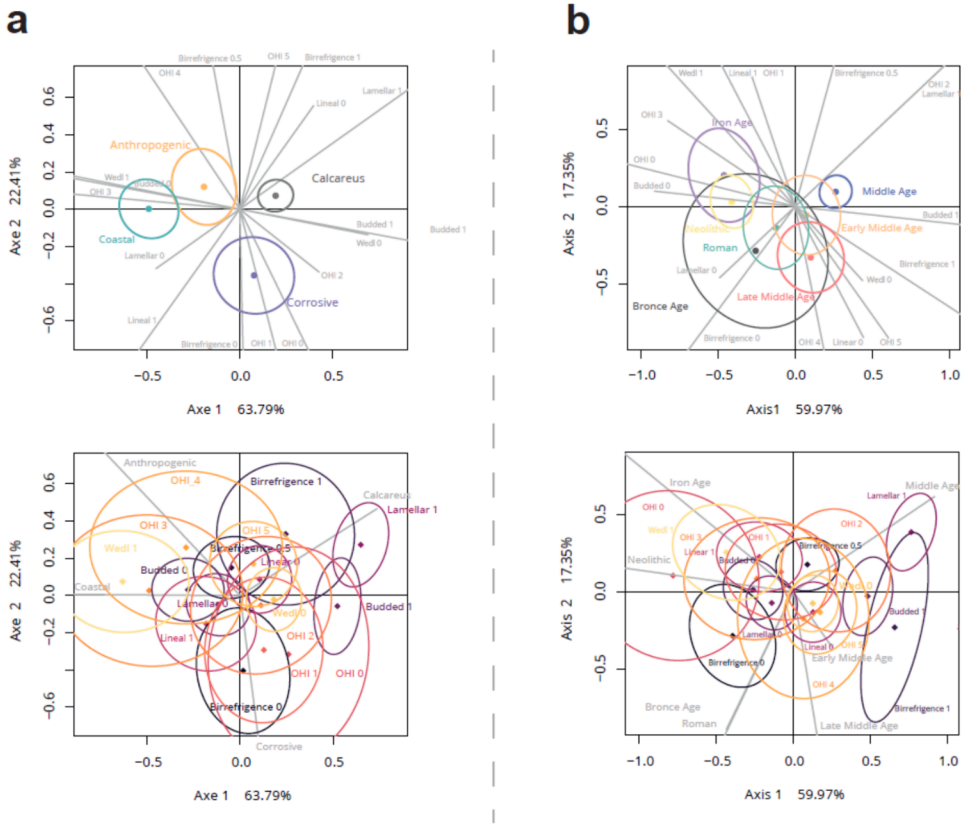

Fig. 9. Multiple Correspondence Analysis taking into account thin section variables. a. MCA based on the burial conditions category exposed by Jans 2005 [94]. B) MCA based on the chronology category exposed by Jans 2005 [78].

density to 1.2 g/ml and the apparent density kept at 2 g/ml. Compared to Pleistocene Azokh Cave, it is noted that the apparent density of these latter samples increases to a greater extent. At the Azokh 1 level, the apparent density can reach values between 2.20–2.5 g/ml, which indicates better preservation values.

MIP intrusion volume data is much higher in BB samples than in other reported cases of less ancient samples, like the Middle Pleistocene Azokh or the ones from some European sites dated between 6000 BP and 200 BP [48,74]. In more recent sites than BB or Azokh Cave, high bone porosities have also been observed. Nielsen-Marsh and Hedges (1999) reported high porosity in Anglo-Saxon bovine bones and Neolithic bones from France. The fluvial nature of these sites suggests some similarity with the deltaic context of BB. Therefore, we cannot assert that high porosity is exclusive to ancient bones; rather, it is influenced by factors

such as burial conditions, soil chemistry, and exposure to water regime [57,70,73,104,111–113].

Variables extracted from histological analysis such as the OHI, presence of microbial attack, or cracking can be used to link the state of preservation with site conditions or chronology. Jans, 2005 [96; pp. 31–40] presents histological data from 40 different archaeological sites across different European countries, detailing their burial conditions (pH, hydrological regime, sediment) and chronologies. These data were analyzed through Multiple correspondence analysis (MCA), providing a relationship between the preservation with buried conditions or chronological ages.

MCA based on buried condition is described in Fig. 9**.a** with Jans 2005 data [81]. This analysis reveals that sites with corrosive conditions exhibit poorer preservation, characterized by low OHI values, absence of birefringence, and presence of bacterial tunnels. These sites typically have acidic pH and permeable sediments, allowing water movement and oxygen ingress. Conversely, calcareous environments demonstrate better preservation, with higher OHI values, the presence of birefringence, and the absence of linear fractures extending through the tissue. However, budded and lamellar fractures, indicative of early alteration stages, are observed.

Coastal and anthropogenic environments exhibit certain trends, with anthropogenic environments generally showing better preservation. Coastal environments, often near or occasionally underwater, display moderate OHI values and a notable presence of fungal-caused Wedl fractures, associated with moist or submerged conditions. Despite some overlap in trends between coastal and anthropogenic environments, the latter typically have better preservation, associated with anoxic conditions and the presence of organic or clayey materials.

Based on these categorizations, it is deduced that the samples from BB are associated with corrosive environments, as evidenced by their histological preservation characteristics. This is consistent with the constantly renewing water environment affecting the bones. These corrosion indicators have been observed in previous studies on other sites of BB in the Mine; however, the preservation of bone surfaces in Pit 1 has not been examined as thoroughly as in this study.

MCA based on chronological category is illustrated in Fig. 9**. b**. Although medieval sites tend to show better preservation, older sites, especially those from the Bronze Age, exhibit greater variability and overlap with Neolithic, Roman, Iron Age, and even some medieval sites. The clear differentiation observed by buried conditions becomes diluted by the chronology variable. This suggests that while age may play a role in preservation, site conditions are more critical in determining the degree of bone conservation.

Although these samples are from older sites, we have already seen that some data, such as porosity, can be similar to recent site data [80]. Therefore, relying solely on the chronology (based on whether it is older or more recent) of the bone samples for a complete characterization of microstructural preservation may provide an incomplete picture. This particular observation has only been reported in a few prior studies on the conservation of archaeological bone [28,31,34].

5. Conclusions

A complete methodology to characterize bone nature by applying diagenesis methodology highlight the significant impact of high porosity, due to bacterial activity, and accelerated collagen hydrolysis, especially in open-site conditions, which pose substantial challenges to preservation efforts. Furthermore, chemical characterization has revealed notable transformations, including the potential recrystallization of bioapatite into fluorapatite and a decrease in organic content. Furthermore, the availability of published data in literature has allowed us to compare Pit 1 at BB samples with a wide range of bones and fossils. Consequently, it suggests that future studies on bone conservation should prioritize a comprehensive diagnosis of the bone sample's nature, as this could be a decisive variable in conservation research.

Last data from Pit 1 at BB from Pit 1 at BB indicate poor bone preservation, correlating qualitative observations with quantitative data regarding porosity and the preservation of chemical bone compounds. These insights have identified that the most significant indicator of deterioration in these bones is primarily due to high porosity, which has underscored the importance of treatments such as consolidation for ensuring the preservation of structural stability.

Moreover, while chemical data on the chemical composition have shown potential significant differences compared to more modern bones or those from different burial contexts, these cannot be directly associated with the preservation of the structure. However, it is crucial to consider these factors in future studies, for instance, during cleaning processes, since bioapatite and fluorapatite exhibit different solubility rates, and the presence or absence of compounds like collagen, carbonates, etc., can directly relate to by-products that may form after treatments such as consolidation, as indicated in the literature.

In conclusion, our study bridges this gap by focusing on characterizing bone preservation through the integration of diagenetic methodologies, evaluating the state of conservation of archaeological bones, and providing foundational analysis for future conservation strategies.

CRediT authorship contribution statement

Andrea Díaz-Cortés: Writing – review & editing, Writing – original draft, Visualization, Methodology, Investigation, Formal analysis, Data curation, Conceptualization. **Héctor Del Valle:** Writing – review & editing, Validation, Supervision, Methodology, Investigation, Data curation. **Lucía López-Polín:** Writing – review & editing, Visualization, Validation, Supervision, Investigation. **Jorge Otero:** Writing – review & editing, Supervision, Methodology, Investigation. **Isabel Cáceres:** Writing – review & editing, Validation, Methodology. **Noé Valtierra:** Writing – review & editing, Visualization, Data curation. **Antonio Pineda:** Writing – review & editing, Visualization, Validation. **Palmira Saladié:** Writing – review & editing, Resources, Project administration. **Josep Vallverdú:** Resources, Project administration.

Declaration of competing interest

The authors declare that they have no known competing financial interests or personal relationships that could have appeared to influence the work reported in this paper.

Data availability

Data will be made available on request.

Acknowledgments

A.D. is funded by an FPU grant (FPU17-05506) from Spanish Ministry of Science, Innovaton and Universities. H D.V research was supported by the Spanish Ministry of Science and Innovation through FPI Fellowship (PRE2021-100275). NV is supported with a FI PhD research fellowship (2021 FI-3 00161) from AGAUR/FSE. A. P is supported by the LATEUROPE project (Grant agreement ID 101052653) that has received funding from the European Research Council (ERC) under the European Union's HORIZON1.1 research program. This work was developed within the frame of the projects: MICINN-PID2021-122355NB-C32, 2021 SGR 01238 and 2023 SGR 01239 (AGAUR), the 2023PFR-URV-01238 and 2023PFR-URV-01239 (URV), and CLT009/18/00053 (DGABMP, Generalitat de Catalunya). Research at IPHES is framed within the CERCA program. The IPHES-CERCA has received financial support from the Spanish Ministry of Science and Innovation through the "María de Maeztu" program for Units of Excellence (CEX2019-000945-M). AD. would like to thanks to Alejandro Rodriguez-Navarro for XRD and thin layers support and Carlos Rodriguez-Navarro for MIP facilities and support provided by the Department of Mineralogy

and Petrology from UGR. AD, also would like to recognized the illustration work by Elisa Díaz Cortés for the graphical abstract.

References

[1] S. Zervos, I. Alexopoulou, Paper conservation methods: a literature review, Cellulose. 22 (2015) 2859–2897, https://doi.org/10.1007/s10570-015-0699-7.

[2] D. Hunt, Properties of wood in the conservation of historical wooden artifacts, J. Cult. Herit. 13 (2012) S10–S15, https://doi.org/10.1016/j.culher.2012.03.014.

[3] E. Doehne, C.A. Price, Stone Conservation An Overview of Current Research, 2010.

[4] A. Moncrieff, G. Weaver, J. Ashley-Smith, Science for Conservators, Vol. 1, An Introduction to Materials, Conservation Science Teaching Series, 1992.

[5] J. Ashurst, Conservation of Building and Decorative Stone, in: Ser. Conserv. Museol., n.d.

[6] J. Ashurst, N. Ashurst, Practical Building Conservation. Vol 1, in: H. Press (Ed.), Stone Masonry, English Herit. Tech. Handb, New York, 1988.

[7] J.M. Cronyn, The Elements of Archaeological Conservation, London (1990), https://doi.org/10.2307/1506325.

[8] J. Ashley-Smith, Science for Conservators, Routledge, An Introduction to materials, 1983.

[9] J.S. Mills, R. White, The organic chemistry of museum objects, 1994.

[10] C.A. Price, Getty Conservation Institute., Stone conservation : an overview of current research, Getty Conservation Institute, Santa Monica CA (1996).

[11] A. Vila, A. Murrays, eds., Diagnosis. Before, During, After, Valencia, 2022. doi: 10.4995/360.2022.657201.

[12] L. López-Polín, Interventive conservation treatments (or preparation) of Pleistocene bones: Criteria for covering information from the archaeopalaeontological record, Quat. Int. 388 (2015) 199–205, https://doi.org/10.1016/j.quaint.2015.05.031.

[13] L. López-Polín, J.M. Bermúdez de Castro, E. Carbonell, The preparation and conservation treatments of the human fossils from Lower Pleistocene unit TD6 (Gran Dolina site, Atapuerca) – The 2003–2009 record, Quat. Int. 433 (2017) 251–262, https://doi.org/10.1016/j.quaint.2015.09.036.

[14] P.S. Storch, Field and Laboratory Methods for Handling Osseous Materials, Conservation, Notes. 6 (1983) 1–8.

[15] G.G. Beiner, R. Rabinovich, An elephant task—conservation of elephant remains from Revadim Quarry, Israel, J. Inst. Conserv. 36 (2013) 56–64, https://doi.org/10.1080/19455224.2013.796887.

[16] L. López-Polín, Possible interferences of some conservation treatments with subsequent studies on fossil bones: A conservator's overview, Quat. Int. 275 (2012) 120–127, https://doi.org/10.1016/j.quaint.2011.07.039.

[17] T.G. Bromage, Interpretation of scanning electron microscopic images of abraded forming bone surfaces, Am. J. Phys. Anthropol. 64 (1984) 161–178, https://doi.org/10.1002/ajpa.1330640210.

[18] L.A. Wiest, J.V. Ferraro, K.M. Binetti, S.L. Forman, D.A. Esker, M. Kibunjia, J.-P. Brugal, B. Zechmann, Morphological characteristics of preparator air-scribe marks: Implications for taphonomic research, PLoS One. 13 (2018) e0209330.

[19] N. Valtierra, A. Díaz-Cortés, L.A. Courtenay, A. Fabregat-Sanjuan, L. López-Polín, Microscopic modifications produced by mechanical cleaning interventions on archaeological bone, J. Cult. Herit. 55 (2022) 107–116, https://doi.org/10.1016/j.culher.2022.03.001.

[20] N. Valtierra, L.A. Courtenay, L. López-Polín, Microscopic analyses of the effects of mechanical cleaning interventions on cut marks, Archaeol. Anthropol. Sci. 12 (2020), https://doi.org/10.1007/s12520-020-01153-8.

[21] C.A.M. France, J.A. Giaccai, C.R. Doney, Brief Communication : The Effects of Paraloid B-72 and Butvar B-98 Treatment and Organic Solvent Removal on d 13 C , d 15 N , and d 18 O Values of Collagen and Hydroxyapatite in a Modern Bone, 338 (2015) 330–338. doi: 10.1002/ajpa.22697.

[22] C.M. Takahashi, D.E. Nelson, J.S. Southon, Radiocarbon and stable isotope anayses of archaeological bone consolidated with hide glue, Arizona Board of Regents (University of Arizona), 2002. https://journals.uair.arizona.edu/index.php/radiocarbon/article/view/4079 (accessed 31 July 2019).

[23] K.M. Moore, M.L. Murray, M.J. Schoeninger, Dietary reconstruction from bones treated with preservatives, J. Archaeol. Sci. 16 (1989) 437–446, https://doi.org/10.1016/0305-4403(89)90018-6.

[24] F. Brock, M. Dee, A. Hughes, C. Snoeck, R. Staff, C. Bronk Ramsey, Testing the Effectiveness of Protocols for Removal of Common Conservation Treatments for Radiocarbon Dating, Radiocarbon. 60 (2018) 35–50, https://doi.org/10.1017/RDC.2017.68.

[25] C.A.M. France, J.A. Giaccai, N. Cano, The effects of PVAc treatment and organic solvent removal on δ13C, δ15N, and δ18O values of collagen and hydroxyapatite in a modern bone, J. Archaeol. Sci. 38 (2011) 3387–3393, https://doi.org/10.1016/j.jas.2011.07.024.

[26] R.A.G. Reid, M.M.E. Jans, L.A. Chesson, R.J. Taylor, G.E. Berg, D. Pow, M.I. A. Accounting, A. Dpaa, M. St, J.B.P. Harbor-hickam, The influence of taphonomy on histological and isotopic analyses of treated and untreated buried modern human bone ☆, J. Archaeol. Sci. 161 (2024) 105901 https://doi.org/10.1016/j.jas.2023.105901.

[27] I.A. Law, R.A. Housley, N. Hammond, R.E.M. Hedges, Cuello: Resolving the Chronology Through Direct Dating of Conserved and Low-Collagen Bone by AMS [1], Radiocarbon. 33 (1991) 303–315, https://doi.org/10.1017/S0033822200040339.

[28] F. Porpora, V. Zaro, L. Liccioli, A. Modi, A. Meoli, G. Marradi, S. Barone, S. Vai, L. Dei, D. Caramelli, M. Fedi, M. Lari, E. Carretti, Performance of innovative nanomaterials for bone remains consolidation and effect on 14C dating and on palaeogenetic analysis, Sci. Rep. 12 (2022) 1–16, https://doi.org/10.1038/s41598-022-10798-5.

[29] J.A. Eklund, The effects of preparation and conservation treatments on DNA., University College of London, 2007.

[30] J.A. Eklund, M.G. Thomas, Assessing the effects of conservation treatments on short sequences of DNA in vitro, J. Archaeol. Sci. 37 (2010) 2831–2841, https://doi.org/10.1016/j.jas.2010.06.019.

[31] A. Salvatore, S. Vai, S. Caporali, D. Caramelli, M. Lari, E. Carretti, Evaluation of Diammonium hydrogen phosphate and Ca(OH)2 nanoparticles for consolidation of ancient bones, J. Cult. Herit. (2019), https://doi.org/10.1016/j.culher.2019.07.022.

[32] L.A. Kres, N.C. Lovell, A Comparison of Consolidants for Archaeological Bone, J. f. Archaeol. 22 (1995) 508–515, https://doi.org/10.1179/009346995791974134.

[33] G. Chaumat, K. Müller, I. Reiche, Preliminary Experiments on Model Artificially Altered Samples to Consolidate Degraded and Wet Archaeological Bone with Azelaic Acid, ArchéoSciences. (2011) 213–222. doi: 10.4000/archeosciences.3219.

[34] I. Natali, P. Tempesti, E. Carretti, M. Potenza, S. Sansoni, P. Baglioni, L. Dei, Aragonite Crystals Grown on Bones by Reaction of CO_2 with Nanostructured Ca $(OH)_2$ in the Presence of Collagen, Implications in Archaeology and Paleontology, Langmuir. 30 (2014) 660–668, https://doi.org/10.1021/la404085v.

[35] A. North, M. Balonis, I. Kakoulli, Biomimetic hydroxyapatite as a new consolidating agent for archaeological bone, Stud. Conserv. (2016), https://doi.org/10.1179/2047058415Y.0000000020.

[36] A.P.F. Pinto, J.D. Rodrigues, Stone consolidation: The role of treatment procedures, J. Cult. Herit. 9 (2008) 38–53, https://doi.org/10.1016/j.culher.2007.06.004.

[37] G. Borsoi, B. Lubelli, R. van Hees, R. Veiga, A. Santos Silva, Evaluation of the effectiveness and compatibility of nanolime consolidants with improved properties, Constr. Build. Mater. 142 (2017) 385–394, https://doi.org/10.1016/j.conbuildmat.2017.03.097.

[38] G. Borsoi, B. Lubelli, R. van Hees, R. Veiga, A.S. Silva, L. Colla, L. Fedele, P. Tomasin, Effect of solvent on nanolime transport within limestone: How to improve in-depth deposition, Colloids Surfaces A Physicochem. Eng. Asp. 497 (2016) 171–181, https://doi.org/10.1016/j.colsurfa.2016.03.007.

[39] G. Borsoi, B. Lubelli, R. van Hees, R. Veiga, A.S. Silva, Understanding the transport of nanolime consolidants within Maastricht limestone, J. Cult. Herit. 18 (2016) 242–249, https://doi.org/10.1016/j.culher.2015.07.014.

[40] E. Rothert, T. Eggers, J. Cassar, J. Ruedrich, B. Fitzner, S. Siegesmund, Stone properties and weathering induced by salt crystallization of Maltese Globigerina Limestone, Geol. Soc. Spec. Publ. 271 (2007) 189–198, https://doi.org/10.1144/GSL.SP.2007.271.01.19.

[41] T. Mifsud, J. Cassar, The treatment of weathered Globigerina Limestone: the surface conversion of calcium carbonate to calcium oxalate, in: Heritage, Weather. Conserv. Proc. Int. Conf. Heritage, Weather. Conserv., 2003: pp. 724–734.

[42] E. Franzoni, E. Sassoni, G. Graziani, Brushing, poultice or immersion? The role of the application technique on the performance of a novel hydroxyapatite-based consolidating treatment for limestone, J. Cult. Herit. 16 (2015) 173–184, https://doi.org/10.1016/j.culher.2014.05.009.

[43] E. Franzoni, G. Graziani, E. Sassoni, G. Bacilieri, M. Griffa, P. Lura, E. Franzoni, G. Graziani, Á.E. Sassoni, Á.G. Bacilieri, M. Griffa, Á.P. Lura, Solvent-based ethyl silicate for stone consolidation: influence of the application technique on penetration depth, efficacy and pore occlusion, Mater. Struct. 48 (2015) 3503–3515, https://doi.org/10.1617/s11527-014-0417-1.

[44] A. Díaz-Cortés, L. López-Polín, J. Otero, Multi-analytical approach for the preservation of Pleistocene bones: evaluation of potential consolidation products and application methods, Microsc. Microanal. 1–16 (2022).

[45] A. Díaz-Cortés, G. Graziani, M. Boi, L. López-Polín, E. Sassoni, Conservation of Archaeological Bones : Assessment of Innovative Phosphate Consolidants in Comparison with Paraloid B72, Nanomaterials. 12 (2022).

[46] F. Porpora, V. Zaro, L. Liccioli, A. Modi, G. AlMeoli, S. Marradi, S. Barone, L. Vai, D. Dei, M. Caramelli, M. Fedi, E.C. Lari, Performance of innovative nanomaterials for bone remains consolidation and effect on 14C dating and on palaeogenetic analysis, Sci. Rep. 12 (2022) 1–16, https://doi.org/10.1038/s41598-022-10798-5.

[47] G. Abdel-Maksoud, R. Sobh, A. Tarek, S.H. Samaha, Evaluation of some pastes used for gap filling of archaeological bones, Meas. J. Int. Meas. Confed. 128 (2018) 284–294, https://doi.org/10.1016/j.measurement.2018.06.061.

[48] C.I. Smith, C.M. Nielsen-Marsh, M.M.E. Jans, M.J. Collins, Bone diagenesis in the European Holocene I: patterns and mechanisms, J. Archaeol. Sci. 34 (2007) 1485–1493, https://doi.org/10.1016/j.jas.2006.11.006.

[49] R.E.M. Hedges, Bone diagenesis: An overview of processes, Archaeometry. 44 (2002) 319–328, https://doi.org/10.1111/1475-4754.00064.

[50] C. Kendall, A.M.H. Eriksen, I. Kontopoulos, M.J. Collins, G. Turner-Walker, Diagenesis of archaeological bone and tooth, Palaeogeogr. Palaeoclimatol. Palaeoecol. 491 (2018) 21–37, https://doi.org/10.1016/j.palaeo.2017.11.041.

[51] I. Kontopoulos, K. Penkman, V.E. Mullin, L. Winkelbach, M. Unterländer, A. Scheu, S. Kreutzer, H.B. Hansen, A. Margaryan, M.D. Teasdale, B. Gehlen, M. Street, N. Lynnerup, I. Liritzis, A. Sampson, C. Papageorgopoulou, M. E. Allentoft, J. Burger, D.G. Bradley, M.J. Collins, Screening archaeological bone

for palaeogenetic and palaeoproteomic studies, PLoS One. 15 (2020) 1–17, https://doi.org/10.1371/journal.pone.0235146.
[52] I. Kontopoulos, K. Penkman, I. Liritzis, M.J. Collins, Bone diagenesis in a Mycenaean secondary burial (Kastrouli, Greece), Archaeol, Anthropol. Sci. 11 (2019) 5213–5230, https://doi.org/10.1007/s12520-019-00853-0.
[53] L. Gatti, F. Lugli, G. Sciutto, M. Zangheri, S. Prati, M. Mirasoli, S. Silvestrini, S. Benazzi, T. Tütken, K. Douka, C. Collina, F. Boschin, M. Romandini, P. Iacumin, M. Guardigli, A. Roda, R. Mazzeo, Combining elemental and immunochemical analyses to characterize diagenetic alteration patterns in ancient skeletal remains, Sci. Rep. 12 (2022) 1–14, https://doi.org/10.1038/s41598-022-08979-3.
[54] S.R. Fernández Lopez, Y. Fernández-Jalvo, The limit between biostratinomy and fossildiagenesis, Curr. Top. Taphon. Foss. (2002) 27–36.
[55] A.K. Behrensmeyer, R. Taphonomy, Modul. Earth Syst, Environ. Sci. (2020) 1–11, https://doi.org/10.1016/b978-0-08-102908-4.00120-x.
[56] M.J. Collins, C. Nielsen-Marsh, J. Hiller, C.I. Smith, J.P. Roberts, R. V. Prigodich, T. Wess, J. Csapo, A.J. Millard, G. Turner-Walker, Bone Diagenesis: implications for heritage management, in: 9th ICAZ Conf., 2002: pp. 124–132.
[57] G. Turner-Walker, Degradation pathways and conservation strategies for ancient bone from wet anoxic sites, Proc. 10th ICOM Gr. Wet Org. Archaeol. Mater. Conf. Amsterdam 2007. (2007) 659–675.
[58] A. Torrisi, E. Proverbio, A. Serra, Ancient Bones Characterization and Preparation Through Freeze-Drying Process, Int. J. Thermophys. 43 (2022) 1–14, https://doi.org/10.1007/s10765-022-03054-5.
[59] G.P. Brophy, J.T. Nash, Compositional, infrared, and X-ray analysis of fossil bone, Am. Mineral. 53 (1968) 445–453.
[60] J.B. Lamberta, J.M. Weydert, S.R. William, J.E. Buikstra, Comparison of Methods for the Removal of Diagenetic Material in Buried Bone, (1990).
[61] J.G. Beeley, D.A. Lunt, The nature of the biochemical changes in softened dentine from archaeological sites, J. Archaeol. Sci. 7 (1980) 371–377, https://doi.org/10.1016/S0305-4403(80)80042-2.
[62] C.C. Gordon, J.E. Buikstra, Soil pH, Bone Preservation, and Sampling Bias at Mortuary Sites, Am. Antiq. 31 (1981) 303–312, https://doi.org/10.1017/s0002731600088764.
[63] R.L. Lyman, Bone density and differential survivorship of fossil classes, J. Anthropol. Archaeol. 3 (1984) 259–299, https://doi.org/10.1016/0278-4165(84)90004-7.
[64] H. Piepenbrink, Two examples of biogenous dead bone decomposition and their consequences for taphonomic interpretation, J. Archaeol. Sci. 13 (1986) 417–430, https://doi.org/10.1016/0305-4403(86)90012-9.
[65] L.S. Bell, Palaeopathology and diagenesis: an SEM evaluation of structural changes using backscattered electron imaging, J. Archaeol. Sci. 17 (1990) 85–102, https://doi.org/10.1016/0305-4403(90)90016-X.
[66] M. Dumont, A. Kostka, P.M. Sander, A. Borbely, A. Kaysser-Pyzalla, Size and size distribution of apatite crystals in sauropod fossil bones, Palaeogeogr. Palaeoclimatol. Palaeoecol. 310 (2011) 108–116, https://doi.org/10.1016/j.palaeo.2011.06.021.
[67] M. Greiner, A. Rodríguez-Navarro, M.F. Heinig, K. Mayer, B. Kocsis, A. Göhring, A. Toncala, G. Grupe, W.W. Schmahl, Bone incineration: An experimental study on mineral structure, colour and crystalline state, J. Archaeol. Sci. Reports. 25 (2019) 507–518, https://doi.org/10.1016/j.jasrep.2019.05.009.
[68] M.M. Beasley, E.J. Bartelink, L. Taylor, R.M. Miller, Comparison of transmission FTIR, ATR, and DRIFT spectra: Implications for assessment of bone bioapatite diagenesis, J. Archaeol. Sci. 46 (2014) 16–22, https://doi.org/10.1016/j.jas.2014.03.008.
[69] L. López-Polín, Metodología y criteiros de restauración de restos óseos pleistocenos. El tratamiento de los fósiles humanos de TD6 (Gran Dolina, Sierra de Atapuerca), Universitat Rovira i Virgili (2016).
[70] R.E.M. Hedges, Bone diagenesis: An overview of the processes, Archaeometry. 44 (2002) 319–328.
[71] M.J. Collins, C.M. Nielsen-Marsh, J. Hiller, C.I. Smith, J.P. Roberts, R. V. Prigodich, T.J. Wess, J. Csapò, A.R. Millard, G. Turner-Walker, The survival of organic matter in bone: A review, Archaeometry. 44 (2002) 383–394, https://doi.org/10.1111/1475-4754.t01-1-00071.
[72] G. Turner-Walker, M. Jans, Reconstructing taphonomic histories using histological analysis, Palaeogeogr. Palaeoclimatol. Palaeoecol. 266 (2008) 227–235, https://doi.org/10.1016/j.palaeo.2008.03.024.
[73] M.M.E. Jans, Microscopic destruction of bone, in: J.T. Pokines, E.N. L'Abbé, S.A. Symes (Eds.), Man. Forensic Taphon., 2nd ed., 2022: pp. 23–39.
[74] C.I. Smith, M. Faraldos, Y. Fernández-Jalvo, Bone diagenesis at azokh caves, in: Vertebr. Paleobiol. Paleoanthropology, 2016: pp. 251–269. doi: 10.1007/978-3-319-24924-7_11.
[75] A. Pineda, I. Cáceres, P. Saladié, R. Huguet, J.I. Morales, A. Rosas, J. Vallverdú, Tumbling effects on bone surface modifications (BSM): An experimental application on archaeological deposits from the Barranc de la Boella site (Tarragona, Spain), J. Archaeol. Sci. 102 (2019) 35–47, https://doi.org/10.1016/j.jas.2018.12.011.
[76] A. Pineda, P. Saladié, J.M. Vergès, R. Huguet, I. Cáceres, J. Vallverdú, Trampling versus cut marks on chemically altered surfaces: An experimental approach and archaeological application at the Barranc de la Boella site (la Canonja, Tarragona, Spain), J. Archaeol. Sci. 50 (2014) 84–93, https://doi.org/10.1016/j.jas.2014.06.018.
[77] A. Pineda, P. Saladié, Beyond the Problem of Bone Surface Preservation in Taphonomic Studies of Early and Middle Pleistocene Open-Air Sites, Springer, US (2022), https://doi.org/10.1007/s10816-022-09550-0.
[78] M. Mosquera, P. Saladié, A. Ollé, I. Cáceres, R. Huguet, J.J. Villalaín, A. Carrancho, D. Bourlès, R. Braucher, J. Vallverdú, Barranc de la Boella (Catalonia, Spain): an Acheulean elephant butchering site from the European late Early Pleistocene, J. Quat. Sci. 30 (2015) 651–666, https://doi.org/10.1002/JQS.2800.
[79] J. Vallverdú, P. Saladié, A. Rosas, R. Huguet, I. Cáceres, M. Mosquera, A. Garcia-Tabernero, A. Estalrrich, I. Lozano-Fernández, A. Pineda-Alcalá, Á. Carrancho, J. J. Villalaín, D. Bourlès, R. Braucher, A. Lebatard, J. Vilalta, M. Esteban-Nadal, M. L. Bennàsar, M. Bastir, L. López-Polín, A. Ollé, J.M. Vergés, S. Ros-Montoya, B. Martínez-Navarro, A. García, J. Martinell, I. Expósito, F. Burjachs, J. Agustí, E. Carbonell, Age and Date for Early Arrival of the Acheulian in Europe (Barranc de la Boella, la Canonja, Spain), PLoS One. 9 (2014) e103634.
[80] C.M. Nielsen-Marsh, R.E.M. Hedges, Bone porosity and the use of mercury intrusion porosimetry in bone diagenesis studies, Archaeometry. 41 (1999) 165–174, https://doi.org/10.1111/j.1475-4754.1999.tb00858.x.
[81] M.M.E. Jans, Histological characterisation of diagenetic alteration of archeological bone, Vriije University, 2005.
[82] R.E.M. Hedges, A.R. Millard, A.W.G. Pike, Measurements and relationships of diagenetic alteration of bone from three archaeological sites, J. Archaeol. Sci. 22 (1995) 201–209, https://doi.org/10.1006/jasc.1995.0022.
[83] A. Millard, The deterioration of Bone, in: Handb. Archaeol. Sci., 2001: p. 637.
[84] R.C. Team, R: A language and environment for statistical computing. R Foundation for Statistical, Computing (2022). https://www.r-project.org/.
[85] T.. Ringrose, cabootcrs: Bootstrap Confidence Regions for Correspondence Analysis., (2013). https://cran.r-project.org/package=cabootcrs.
[86] M. Lebon, I. Reiche, X. Gallet, L. Bellot-Gurlet, A. Zazzo, Rapid quantification of bone collagen content by ATR-FTIR spectroscopy, Radiocarbon. 58 (2016) 131–145, https://doi.org/10.1017/RDC.2015.11.
[87] C.A.M. France, N. Sugiyama, E. Aguayo, Establishing a preservation index for bone, dentin, and enamel bioapatite mineral using ATR-FTIR, J. Archaeol. Sci. Reports. 33 (2020) 102551, https://doi.org/10.1016/j.jasrep.2020.102551.
[88] G. Dal Sasso, M. Lebon, I. Angelini, L. Maritan, D. Usai, G. Artioli, Bone diagenesis variability among multiple burial phases at Al Khiday (Sudan) investigated by ATR-FTIR spectroscopy, Palaeogeogr. Palaeoclimatol. Palaeoecol. 463 (2016) 168–179, https://doi.org/10.1016/j.palaeo.2016.10.005.
[89] M. Lebon, I. Reiche, J.J. Bahain, C. Chadefaux, A.M. Moigne, F. Fröhlich, F. Sémah, H.P. Schwarcz, C. Falguères, New parameters for the characterization of diagenetic alterations and heat-induced changes of fossil bone mineral using Fourier transform infrared spectrometry, J. Archaeol. Sci. 37 (2010) 2265–2276, https://doi.org/10.1016/j.jas.2010.03.024.
[90] E. Margariti, E.T. Stathopoulou, Y. Sanakis, E. Kotopoulou, P. Pavlakis, A. Godelitsas, A geochemical approach to fossilization processes in Miocene vertebrate bones from Sahabi, NE Libya, J. African Earth Sci. 149 (2019) 1–18, https://doi.org/10.1016/j.jafrearsci.2018.07.019.
[91] E.T. Stathopoulou, V. Psycharis, G.D. Chryssikos, V. Gionis, G. Theodorou, Bone diagenesis: New data from infrared spectroscopy and X-ray diffraction, Palaeogeogr. Palaeoclimatol. Palaeoecol. 266 (2008) 168–174, https://doi.org/10.1016/j.palaeo.2008.03.022.
[92] H. Rietveld, A profile refinement method for nuclear and magnetic structures, J. Appl. Chem. 2 (1969) 65–71, https://doi.org/10.1107/S0021889869006558.
[93] G. Turner-Walker, C.M. Nielsen-Marsh, U. Syversen, H. Kars, M.J. Collins, Sub-micron Spongiform Porosity is the Major Ultra-structural Alteration Occurring in Archaeological Bone, Int. J. Osteoarchaeol. 12 (2002) 407–414, https://doi.org/10.1002/oa.642.
[94] C.N. Trueman, D.M. Martill, The long-term survival of bone: the role of bioerosion, Archaeometry. 44 (2002) 371–382, https://doi.org/10.1111/1475-4754.t01-1-00070.
[95] S.J. Roberts, C.I. Smith, A. Millard, M.J. Collins, The taphonomy of cooked bone: characterizing boiling and its physico-chemical effects, Archaeometry. 44 (2002) 485–494, https://doi.org/10.1111/1475-4754.t01-1-00080.
[96] G. Turner-walker, PART 1 Analytical Approaches in The Chemical and Microbial Degradation of Bones and Teeth, (2008).
[97] M.M.E. Jans, C.M. Nielsen-Marsh, C.I. Smith, M.J. Collins, H. Kars, Characterisation of microbial attack on archaeological bone, J. Archaeol. Sci. 31 (2004) 87–95, https://doi.org/10.1016/j.jas.2003.07.007.
[98] G. Turner-Walker, Light at the end of the tunnels? The origins of microbial bioerosion in mineralised collagen, Palaeogeogr. Palaeoclimatol. Palaeoecol. 529 (2019) 24–38, https://doi.org/10.1016/j.palaeo.2019.05.020.
[99] T.E. Rudakova, G.E. Zaikov, Degradation of collagen and its possible applications in medicine, Polym. Degrad. Stab. 18 (1987) 271–291, https://doi.org/10.1016/0141-3910(87)90015-2.
[100] M.S. Riley, M.J. Collins, The polymer model of collagen degradation, Polym. Degrad. Stab. 46 (1994) 93–97, https://doi.org/10.1016/0141-3910(94)90113-9.
[101] M. Jackes, Destruction of Microstructure in Archaeological Bone : a Case Study from Portugal, Int. J. Osteoarchaeol. 432 (2001) 415–432, https://doi.org/10.1002/oa.583.
[102] G. Dal Sasso, L. Maritan, D. Usai, I. Angelini, G. Artioli, Bone diagenesis at the micro-scale: Bone alteration patterns during multiple burial phases at Al Khiday (Khartoum, Sudan) between the Early Holocene and the II century AD, Palaeogeogr. Palaeoclimatol. Palaeoecol. 416 (2014) 30–42, https://doi.org/10.1016/j.palaeo.2014.06.034.
[103] Y. Fernández-Jalvo, P. Andrews, Atlas of taphonomic identifications, in: Vertebr. Paleobiol. Paleoanthropology, Springer, 2016: pp. 1–359. doi: 10.1007/978-94-017-7432-1.
[104] C.I. Smith, C.M. Nielsen-Marsh, M.M.E. Jans, P. Arthur, A.G. Nord, M.J. Collins, The strange case of Apigliano: early 'fossilization' of medieval bone in southern

Italy, Archaeometry. 44 (2002) 405–415, https://doi.org/10.1111/1475-4754.t01-1-00073.
[105] G.F. Monnier, A review of infrared spectroscopy in microarchaeology: Methods, applications, and recent trends, J. Archaeol. Sci. Reports. 18 (2018) 806–823, https://doi.org/10.1016/j.jasrep.2017.12.029.
[106] A. Antonakos, E. Liarokapis, T. Leventouri, Micro-Raman and FTIR Studies of Synthetic and Natural Apatites 28 (2007) 3043–3054, https://doi.org/10.1016/j.biomaterials.2007.02.028.
[107] J. Aufort, D. Gommery, C. Gervais, L. Segalen, N. Labourdette, C. Coelho-Diogo, E. Balan, Assessing bone transformation in late Miocene and Plio-Pleistocene deposits of Kenya and South Africa, Archaeometry. 61 (2019) 1129–1143, https://doi.org/10.1111/arcm.12471.
[108] G. Piga, A. Santos-Cubedo, S. Moya Solà, A. Brunetti, A. Malgosa, S. Enzo, An X-ray Diffraction (XRD) and X-ray Fluorescence (XRF) investigation in human and animal fossil bones from Holocene to Middle Triassic, J. Archaeol. Sci. 36 (2009) 1857–1868, https://doi.org/10.1016/j.jas.2009.04.013.
[109] M.B. Kasiri, Fluoride Dating of Skeletons of the Iron Age Cemetery of Tabriz, Iran, Sci. Cult. 6 (2020) 39–48, https://doi.org/10.5281/zenodo.3600580.
[110] C.I. Smith, M. Faraldos, Y. Fernández-Jalvo, The precision of porosity measurements: Effects of sample pre-treatment on porosity measurements of modern and archaeological bone, Palaeogeogr. Palaeoclimatol. Palaeoecol. 266 (2008) 175–182, https://doi.org/10.1016/j.palaeo.2008.03.028.
[111] C.M. Nielsen-Marsh, C.I. Smith, M.M.E. Jans, A. Nord, H. Kars, M.J. Collins, Bone diagenesis in the European Holocene II: taphonomic and environmental considerations, J. Archaeol. Sci. 34 (2007) 1523–1531, https://doi.org/10.1016/j.jas.2006.11.012.
[112] M.M.E. Jans, H. Kars, C.M. Nielsen-Marsh, C.I. Smith, A.G. Nord, P. Arthur, N. Earl, In situ preservation of archaeological bone: A histological study within a multidisciplinary approach, Archaeometry. 44 (2002) 343–352, https://doi.org/10.1111/1475-4754.t01-1-00067.
[113] C.M. Nielsen-Marsh, R.E.M. Hedges, Patterns of diagenesis in bone I: The effects of site environments, J. Archaeol. Sci. 27 (2000) 1139–1150, https://doi.org/10.1006/jasc.1999.0537.